JACS
JOURNAL OF THE AMERICAN CHEMICAL SOCIETY

Communication

pubs.acs.org/JACS

Borane-Catalyzed Room-Temperature Hydrosilylation of Alkenes/Alkynes on Silicon Nanocrystal Surfaces

Tapas K. Purkait,[†] Muhammad Iqbal,[†] Maike H. Wahl,[‡] Kerstin Gottschling,[§] Christina M. Gonzalez,[†] Muhammad Amirul Islam,[†] and Jonathan G. C. Veinot*[,†]

[†]Department of Chemistry, University of Alberta, 11227 Saskatchewan Drive, Edmonton, Alberta Canada T6G 2G2

[‡]Department of Chemistry, Technische Universität München, Lichtenbergstraße 4, 85748 Garching, Germany

[§]Department of Chemistry, Ludwig-Maximilians-Universität München, Butenandtstraße 5-13, 81377 München, Germany

Supporting Information

ABSTRACT: Room-temperature borane-catalyzed functionalization of hydride-terminated silicon nanocrystals (H-SiNCs) with alkenes/alkynes is reported. This new methodology affords formation of alkyl and alkynyl surface monolayers of varied chain lengths (i.e., C_5–C_{12}). The present study also indicates alkynes react more readily with H-SiNC surfaces than equivalent alkenes. Unlike other toxic transition-metal catalysts, borane or related byproducts can be readily removed from the functionalized SiNCs. The new method affords stable luminescent alkyl/alkenyl-functionalized SiNCs.

Silicon is plentiful, and its established applications are vast and impactful; they range from solar cells to electronics. Of late, silicon nanocrystals (SiNCs) have garnered considerable attention, primarily as a result of their unique size and surface chemistry-dependent optoelectronic properties as well as its low cytotoxicity.[1−4] Prototype applications of silicon-based nanomaterials include electronics,[5] photonics,[6,7] photovoltaics,[7,8] and even medicine.[9] To be useful in these and other target areas, SiNCs must be interfaced with their environment (e.g., solubility, chemical linkages, etc.) and stabilized against undesirable reactions (e.g., oxidation) that could lead to unpredictable properties. In this context, methods affording effective SiNC surface passivation are of paramount importance.

The most common approaches toward SiNC surface functionalization employ variations of alkene/alkyne hydrosilylation (*vide infra*) that involve addition of a Si−H bond across an unsaturated carbon−carbon multiple bond. Hence, hydride-terminated SiNCs (H-SiNCs) are an attractive reactive platform for attaching surface groups. The resulting surface bonded moieties are linked through robust covalent Si−C linkages, render SiNCs soluble in common organic solvents, and improve oxidation resistance.[10] Hydrosilylation of unsaturated carbon−carbon bonds by H-SiNCs is commonly achieved by providing thermal[11,12] or photochemical activation[13,14] or can be realized by employing radical initiators[15] and metal-based catalysts.[16,17] Each of these methods has its advantages and limitations. For example, thermal and photochemical methods do not require any additional reagents thereby minimizing impurities. However, while a few exceptions exist,[18,19] thermal hydrosilylation generally requires high reaction temperatures (i.e., 160−190 °C) and high boiling (i.e., long chain) alkenes or alkynes.[20] Further limiting the utility of this approach, our group recently discovered oligomerization of terminal alkenes can occur on SiNC surfaces.[20] Photochemically-induced hydrosilylation is dependent on SiNC size and is relatively slow limiting its utility.[21] On the other hand, while somewhat costly transition-metal catalysts (e.g., H_2PtCl_6) provide efficient low temperature access to surface hydrosilylation, removal of residual metals is difficult and can compromise important material properties (e.g., quench or alter the photoluminescence).[16] It is also reasonable that trace transition metals could render hydrosilylated SiNCs toxic and restrict their future biological and medical applications.[22] Room-temperature diazonium salts-initiated hydrosilylation[23] as well as catalyst-free hydrosilylation[24] of SiNCs have also been reported; in these reactions diazonium salts, oxygen, or oxygen-containing functional groups initiate hydrosilylation.[20]

Despite these impressive advances, key challenges remain in establishing methods that afford effective SiNC surface modification. When designing new functionalization strategies targeted methods should ideally proceed under mild conditions and provide predictable formation of mono- and multilayers on SiNC surfaces, and byproducts should be minimized and/or easily removed.[25]

Lewis acids (e.g., tris(pentafluorophenyl)borane and alkylaluminum chloride) have been investigated as hydrosilylation catalysts in the derivatization of molecular silanes.[26,27] Precedent for applying this approach to nanostructured silicon is provided by Buriak et al., who employed $EtAlCl_2$ to catalyze hydrosilylation of alkenes/alkynes on porous Si.[28] Lewis acid catalysts that promote the modification of molecular substrates do not necessarily exhibit the same reactivity toward Si nanosystems. For example, $(C_6F_5)_3B$ and BF_3, which catalyze hydrosilylation of imines,[29] thioketones,[30] ketones,[31] and alkenes[27] by molecular silanes are ineffective for analogous reactions on porous silicon.[28] To our knowledge, other Lewis acids, such as diborane or BH_3·THF, have not been applied in the surface modification of nanoscale silicon and more specifically in the derivatization of colloidal SiNCs. Borane catalysts are particularly appealing because the catalyst itself as well as the reaction byproducts are readily removed using straightforward procedures.[32] Further-

Received: October 1, 2014
Published: December 10, 2014

ACS Publications © 2014 American Chemical Society

dx.doi.org/10.1021/ja510120e | J. Am. Chem. Soc. 2014, 136, 17914−17917

more, if boron-containing impurities remain they are expected to be biocompatible and/or nontoxic.[32] Herein, we report a rapid room-temperature approach for preparing alkyl-/alkenyl-passivated SiNCs that exploits borane-initiated hydrosilylation of H-SiNCs. The presented procedure provides access to a wide variety of surface ligands, including low boiling volatile alkenes and alkynes, and affords luminescent freestanding SiNCs that are soluble in common organic solvents.

Well-defined H-SiNCs used in the present study were prepared using a well-established procedure developed in the Veinot Laboratory (see Supporting Information, SI).[33] Briefly, an SiNC/SiO_2 composite obtained from reductive thermal processing of commercial hydrogen silsesquioxane (HSQ) was exposed to a hydrofluoric acid etching protocol to remove the oxide matrix and liberate H-SiNCs. The size and shape of these SiNCs may be controlled by defining the thermal processing conditions.[34] A series of representative alkynes and alkenes were chosen to explore the scope of the presented reaction (Scheme 1). Briefly, air-free alkyne or alkene was added to a degassed

Scheme 1. Borane-Catalyzed Functionalization of H-SiNCs To Yield Alkyl/Alkenyl-Passivated SiNCs

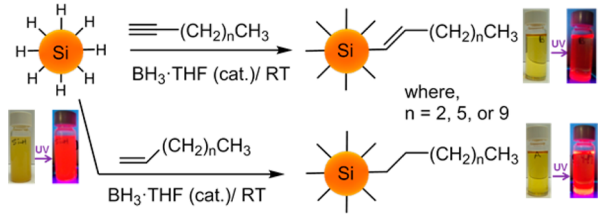

toluene suspension of H-SiNCs, and a catalytic quantity (~2.5 mol % of the ligand) of BH_3·THF was introduced. Following stirring at room temperature for an appropriate time (i.e., 1-alkynes, 30 min; internal alkynes, 12 h, 1-alkenes, 12 h) the opaque reaction mixture yielded a nonopalescent solution of red-emitting surface functionalized SiNCs. The following discussion outlines a detailed evaluation of the resulting surface modified SiNCs as well as the nature of the surface functionalities and their general material properties.

FTIR analysis of the SiNCs provides insight into the nature of the surface groups. The IR spectrum of H-terminated SiNCs shows a characteristic structured feature at ~2100 cm^{-1} that is routinely assigned to Si−H_x (x = 1−3) stretching (Figures S1a and S1c).[18,19]Spectra for functionalized SiNCs are obtained from reactions with alkenes. Figure S1a shows features arising from saturated ν(C−H) stretching at 2850−3000 cm^{-1} and δ(C−H) bending at 1365 and 1475 cm^{-1}. Attachment of surface groups to SiNCs through a Si−C bond is supported by the appearance of a weak absorption at 1258 cm^{-1} arising from symmetric C−H bending (umbrella mode) of Si-CH group as well as a feature at ~800 cm^{-1} that we tentatively assign to Si−C stretching.[35] Spectra acquired for products of reactions with alkynes (See Figure S1b) showed an absorption at 1600 cm^{-1} that we confidently assign to ν(C═C). Other important features appearing in these spectra include absorptions attributable to aliphatic C−H stretching and bending at 2850−2930 and 1475−1365 cm^{-1}, respectively. Spectral features arising from vinyl C−H vibrations are generally of low intensity and appear at ~3040 cm^{-1}; unfortunately, this feature is not obvious in the analysis of the present systems. Broad absorptions are also present in the spectra of all alkene and alkyne-derivatized NCs that are consistent with incomplete surface coverage (*vide infra*) and assigned to OSi-H (~2240 cm^{-1}), SiH_x (~2100 cm^{-1}), and Si−O (~1130−1000 cm^{-1}).[36]

Proton nuclear magnetic resonance (^{1}H NMR) spectroscopy provides valuable information regarding proton environments on surface ligands and more conclusive identification of SiNC surface modification. For example, the ^{1}H NMR spectra of SiNCs functionalized with various alkynes in CD_2Cl_2 (Figure S2) show resonances from terminal methyl protons at ~0.9 ppm and methylene chain protons appearing as a broad peak with chemical shifts in the range of ~1.1 to 1.6 ppm. Features arising from vinylic protons on the nanoparticle surfaces usually appear between ~5 and 6 ppm;[37] however, they were not observed in the present ^{1}H NMR, as these protons were closely associated with the nanocrystal surface. Broadening of ^{1}H NMR resonance peaks of the functionalized SiNCs is expected due to long relaxation times resulting from slow rotation of SiNCs in solution.[37] Despite peak broadening limiting the exact determination of integration ratios, valuable information is still provided from this analysis. For the present systems, the integration ratios of the methyl (at 0.9 ppm) and methylene proton signals was determined to be 3:4.2, 3:10, and 3:18 for 1-pentenyl-, 1-octenyl-, and 1-dodecenyl-functionalized SiNCs, respectively; these data are consistent with expected surface bonded groups. The resonances of 2-octenyl-SiNCs were confirmed by the appearance of features at 0.9 ppm (terminal methyl protons), 1.5 ppm internal methyl protons (bonded to C═C), and at 1.2 to 1.6 ppm for the remaining methylene protons. The ^{1}H NMR spectra of alkene-functionalized SiNCs acquired in CD_2Cl_2 (Figure S3) showed resonances from terminal methyl protons with a chemical shift at 0.9 ppm and methylene protons with chemical shifts in the range of 1.1−1.6 ppm as a broad peak, as expected. The ratio of the integration of the methyl protons (at 0.9 ppm) and the methylene protons were found to be 3:7.5, 3:12, and 3:20 for 1-pentyl, 1-octyl, and 1-dodecyl, respectively.

The degree of SiNC surface coverage achieved from the present reactions was estimated for d = 3.6 nm SiNCs using the ^{1}H NMR and thermogravimetric analysis (TGA) as described by Hua et al.[13] Details of these procedures/calculations are outlined in Tables S1 and S2. Based upon the TEM determined diameter (*vide infra*; $d = 3.6 \pm 0.56$ nm) and that a compact icosohedron is the most stable structure for SiNCs of this dimension,[38] we invoked the estimation that the present NCs adopt this structure and contain 1100 Si atoms (for d = 3.51 nm).[38] A comparison of the integrated peak areas of the surface alkyl or alkenyl groups to an internal standard (i.e., tetramethylsilane) provides an estimate of the number of ligands per NC and percent surface coverage (see Figure S4 and Table S1). Surface coverage determined from these approximations is in agreement with values previously reported for SiNC hydrosilylation reactions[13] and decreases with increased chain length. We also note, alkyne-derived surface coverage is consistently lower.[14] The origin of this difference is the subject of ongoing study. Furthermore, consistent with the increased bulk associated with attaching the 2-octenyl moiety to SiNCs, reactions with 2-octyne provided the lowest surface coverage of those investigated.

Having identified the surface groups on the present NCs we endeavored to confirm the NC core remained intact following reaction. Size and morphology of the functionalized SiNCs were analyzed by TEM and HRTEM. Bright-field TEM images (see Figures S6 and S7) show the functionalized NCs adopt a pseudospherical shape. The average diameter of the functionalized Si NCs is ~3.6 nm. Lattice fringes appearing in HRTEM

dx.doi.org/10.1021/ja510120e | J. Am. Chem. Soc. 2014, 136, 17914−17917

images can be readily attributed the Si(111) lattice spacing (*d*-spacing = 0.32 nm) and confirm SiNCs are crystalline.[39]

Survey X-ray photoelectron spectra (XPS) and electron dispersive X-ray spectra (EDX, not shown) confirm the presence of only Si, C, and trace amounts of O. No boron was detected at the sensitivity of the EDX and XPS methods consistent with effective removal of the catalyst. High-resolution XPS of Si 2p region (Figure 1) shows an intense emission at 99.3 eV

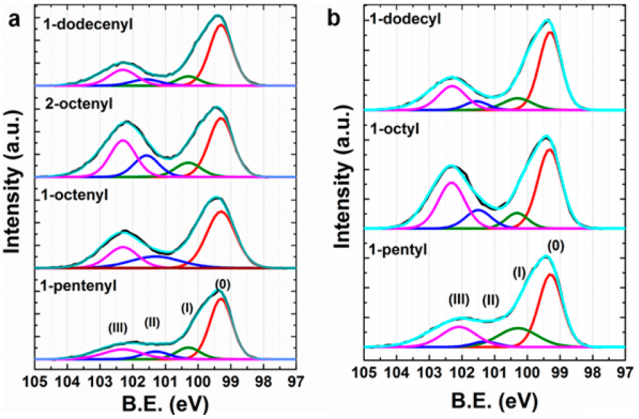

Figure 1. Si 2p region of the high-resolution XP spectra of SiNCs functionalized with indicated surface groups. Fitting is shown for the Si $2p_{3/2}$ component. The Si $2p_{1/2}$ components have omitted for clarity.

characteristic of core Si atoms (i.e., Si(0)); signals arising from Si surface atoms as well as Si suboxides were observed at 100.3, 101.3, 102.3, and 103.4 eV.[20] We note that longer surface groups yield more intense XP signals associated with silicon suboxides. In addition, comparatively intense suboxide signals were detected for SiNCs modified with 2-octyne. These observations are consistent with less effective surface passivation that may be attributed to incomplete functionalization resulting from steric interactions between surface pendant chains (*vide supra*). Interestingly, the Si 2p XP spectra of 1-dodecenyl-SiNCs showed less intense suboxide signals than that observed for corresponding octenyl-SiNCs. While the exact origin of this observation is difficult to identify, it is reasonable the C_{12} chain is long enough to cover and envelop the surface resulting in somewhat improved oxidation resistance. A similar trend was observed for SiNCs functionalized with alkenes (Figure 1b).

To investigate the possibility of size-dependent reactivity of SiNCs toward the present borane-catalyzed hydrosilylation protocol larger SiNCs with average diameters of 5.8 ± 0.72 and 7.5 ± 0.92 nm were evaluated. Representative TEM images, size distribution, and HRTEM images of three different sizes of octyl-SiNCs are shown in Figure 2. Powder X-ray detraction patterns of these functionalized SiNCs (Figure S8) show their crystallinity and the average crystallite sizes consistent with the particle sizes estimated from TEM images. Reactions of larger H-SiNCs were qualitatively slower as evaluated by the appearance of a transparent solution. For example, reactions with 1-octyne required 12, 2, and 0.5 h for SiNCs with d = 7.5, 5.8, and 3.6 nm, respectively. Functionalization of SiNCs with 1-octene is size independent but is qualitatively slower than 1-octyne. As expected, FTIR analyses of all 1-octyne-functionalized SiNCs (Figures S9–S12) confirmed the presence of the target surface functionality showing absorptions at 3000–2800 cm^{-1} for ν(C–H) stretching vibrations and at 1475–1365 cm^{-1} for δ(C–H) bending.

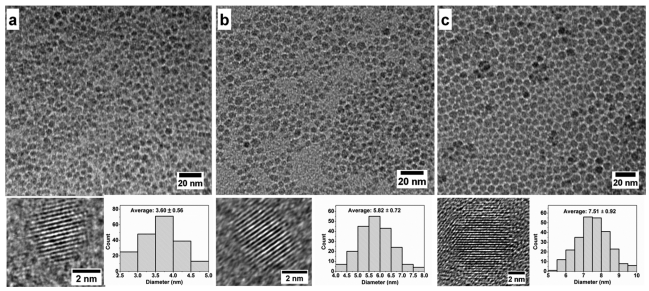

Figure 2. Representative bright-field TEM and HRTEM images and size distributions of octyl-SiNCs of diameter: (a) 3.6, (b) 5.8, and (c) 7.5 nm.

Photoluminescence (PL) of SiNCs functionalized by thermal, photochemical, and catalytic hydrosilylation using alkenes or alkynes has been reported previously.[25] The alkenyl moiety on the Si surface can change PL energy and intensity.[40] For example, when conjugated alkynes (especially arylacetylenes) are tethered to the surface of SiNCs, the PL is quenched.[14,28] Octyl-SiNCs (d = 3.6 ± 0.56 nm) exhibit PL centered at ~694 nm, whereas octenyl-SiNCs with diameter of 3.7 ± 0.57 nm exhibit slightly red-shifted PL centered at 702 nm (Figure S13). PL intensity of SiNCs with alkenyl-moieties showed decreased PL intensities compared to their alkyl-SiNCs counterparts which is attributed to conjugation of C=C with SiNC surfaces. Both octyl- and octenyl-SiNCs show PL lifetimes of 113 and 125 μs, respectively (Figures S14 and S15) consistent with indirect band gap and comparable with that previously reported for SiNCs.[41] Octyl-SiNCs (d = 5.8 ± 0.72 and 7.5 ± 0.92 nm) exhibit size-dependent PL with emission maxima at 756 and 935 nm, respectively (Figure S16).

Lewis acid-catalyzed hydrosilylation of alkenes and alkynes has been reported previously for molecular silanes and H-terminated porous Si.[27−29,42,43] In 1985, Oertle et al. proposed $AlCl_3$-catalyzed hydrosilylation proceeds via hydroalumination of the alkene via a hydroalane intermediate, followed by transmetalation of the resulting alkylalane with hydrosilane.[42] In contrast, $(C_6F_5)_3B$ is believed to catalyze the hydrosilylation reaction via activation of Si–H bond forming a silylium cation.[27,44] This mechanism may not be active Si-based nanomaterials because $(C_6F_5)_3B$ was ineffective for the present H-SiNCs and in a previous study involving H-terminated porous Si.[28] Furthermore, attempts to activate the H-SiNC surfaces with BH_3·THF followed by subsequent addition of alkene/alkyne provided no functionalization. In this context, we propose hydrosilylation in the present system proceeds via a mechanism similar to that outlined for $AlCl_3$ involving the formation a hydroboration product (Scheme 2, Pathway A) or direct activation of the alkene/alkyne (Scheme 2, Pathway B). For Pathway A, an intermediate **A-II** is formed from the reaction of

Scheme 2. Proposed Mechanism of Borane-Catalyzed Functionalization of H-SiNCs Using Alkenes/Alkynes

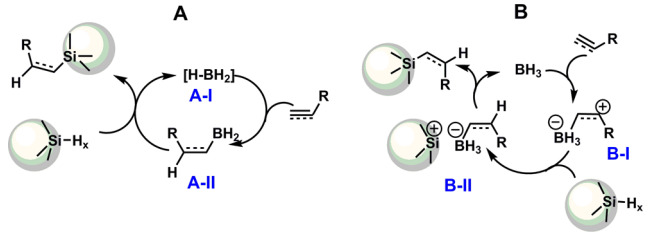

dx.doi.org/10.1021/ja510120e | J. Am. Chem. Soc. 2014, 136, 17914–17917

BH_3·THF with alkene/alkyne, followed by insertion of the intermediate **A-II** to Si−H bond. For Pathway B, an activated complex **B-I** is formed from direct activation of the alkene/alkyne by BH_3·THF, followed by formation of a complex (**B-II** in Scheme 2) from the reaction of activated complex **B-I** and H-SiNCs. Further elucidation of this mechanism is the subject of ongoing investigation.

In conclusion, this work presents an efficient room-temperature functionalization of SiNCs using various alkenes and alkynes via borane-catalyzed hydrosilylation. The alkyl/alkenyl functionality with C_5 to C_{12} chains was confirmed by FTIR and ^{1}H NMR spectroscopy. Estimates of surface coverage obtained from ^{1}H NMR spectroscopy and TGA indicate functionalization is more effective when shorter, terminal ligands are employed. SiNCs (d = 3.6 nm) with alkyl functionalization show orange-red PL, and a decrease in PL intensity was observed in alkenyl-functionalized SiNCs due to C═C bond conjugation.

■ ASSOCIATED CONTENT

Supporting Information

Experimental details and characterization data. This material is available free of charge via the Internet at http://pubs.acs.org.

■ AUTHOR INFORMATION

Corresponding Author

jveinot@ualberta.ca

Notes

The authors declare no competing financial interest.

■ ACKNOWLEDGMENTS

The authors recognize NSERC for continued generous support. Dr. Al Meldrum, Stephen Lane, and Rose Chung are thanked for the assistance with PL lifetime measurements. Kai Cui (NINT) and D. Karpuzav (ACSES) are also thanked for assistance with HRTEM and XPS analysis, respectively. Thanks are conveyed to all Veinot Team members including former group members Dr. Mita Dasog and Dr. Zhenyu Yang for their thoughtful and insightful discussions. The authors acknowledge Dr. Eric Rivard and Olena Shynkaruk for TGA measurement.

■ REFERENCES

(1) Erogbogbo, F.; Yong, K.-T.; Roy, I.; Hu, R.; Law, W.-C.; Zhao, W.; Ding, H.; Wu, F.; Kumar, R.; Swihart, M. T.; Prasad, P. N. *ACS Nano* **2011**, *5*, 413−423.

(2) Park, J.-H.; Gu, L.; von Maltzahn, G.; Ruoslahti, E.; Bhatia, S. N.; Sailor, M. *J. Nat. Mater.* **2009**, *8*, 331−336.

(3) McVey, B. F. P.; Tilley, R. D. *Acc. Chem. Res.* **2014**, *47*, 3045−3051.

(4) Dasog, M.; De los Reyes, G. B.; Titova, L. V.; Hegmann, F. A.; Veinot, J. G. C. *ACS Nano* **2014**, *8*, 9636−9648.

(5) Ding, Y.; Dong, Y.; Bapat, A.; Nowak, J. D.; Carter, C. B.; Kortshagen, U. R.; Campbell, S. A. *IEEE Trans. Electron Devices* **2006**, *53*, 2525−2531.

(6) Walters, R. J.; Bourianoff, G. I.; Atwater, H. A. *Nat. Mater.* **2005**, *4*, 143−146.

(7) Priolo, F.; Gregorkiewicz, T.; Galli, M.; Krauss, T. F. *Nat. Nanotechnol.* **2014**, *9*, 19−32.

(8) Perez-Wurfl, I.; Hao, X.; Gentle, A.; Kim, D.-H.; Conibeer, G.; Green, M. A. *Appl. Phys. Lett.* **2009**, *95*, 153506−3.

(9) Regli, S.; Kelly, J. A.; Barnes, M. A.; Andrei, C. M.; Veinot, J. G. C. *Mater. Lett.* **2014**, *115*, 21.

(10) Linford, M. R.; Chidsey, C. E. D. *J. Am. Chem. Soc.* **1993**, *115*, 12631−12632.

(11) Linford, M. R.; Fenter, P.; Eisenberger, P. M.; Chidsey, C. E. D. *J. Am. Chem. Soc.* **1995**, *117*, 3145−3155.

(12) Boukherroub, R.; Morin, S.; Bensebaa, F.; Wayner, D. D. M. *Langmuir* **1999**, *15*, 3831−3835.

(13) Hua, F.; Swihart, M. T.; Ruckenstein, E. *Langmuir* **2005**, *21*, 6054−6062.

(14) Kelly, J. A.; Veinot, J. G. C. *ACS Nano* **2010**, *4*, 4645−4656.

(15) Nelles, J.; Sendor, D.; Ebbers, A.; Petrat, F. M.; Wiggers, H.; Schulz, C.; Simon, U. *Colloid Polym. Sci.* **2007**, *285*, 729−736.

(16) Holland, J. M.; Stewart, M. P.; Allen, M. J.; Buriak, J. M. *J. Solid State Chem.* **1999**, *147*, 251−258.

(17) Warner, J. H.; Hoshino, A.; Yamamoto, K.; Tilley, R. D. *Angew. Chem., Int. Ed.* **2005**, *44*, 4550−4554.

(18) Weeks, S. L.; Macco, B.; van de Sanden, M. C. M.; Agarwal, S. *Langmuir* **2012**, *28*, 17295−17301.

(19) Jariwala, B. N.; Dewey, O. S.; Stradins, P.; Ciobanu, C. V.; Agarwal, S. *ACS Appl. Mater. Interfaces* **2011**, *3*, 3033−3041.

(20) Yang, Z.; Iqbal, M.; Dobbie, A. R.; Veinot, J. G. C. *J. Am. Chem. Soc.* **2013**, *135*, 17595−17601.

(21) Kelly, J. A.; Shukaliak, A. M.; Fleischauer, M. D.; Veinot, J. G. C. *J. Am. Chem. Soc.* **2011**, *133*, 9564−9571.

(22) Lambert, J. M. J. *Biomed. Mater. Res., Part B* **2006**, *78B*, 167−180.

(23) Hoehlein, I. M. D.; Kehrle, J.; Helbich, T.; Yang, Z.; Veinot, J. G. C.; Rieger, B. *Chem.—Eur. J.* **2014**, *20*, 4212−4216.

(24) Yu, Y.; Hessel, C. M.; Bogart, T. D.; Panthani, M. G.; Rasch, M. R.; Korgel, B. A. *Langmuir* **2013**, *29*, 1533−1540.

(25) Veinot, J. G. C. *Chem. Commun.* **2006**, 4160−4168.

(26) Song, Y.-S.; Yoo, B. R.; Lee, G.-H.; Jung, I. N. *Organometallics* **1999**, *18*, 3109−3115.

(27) Rubin, M.; Schwier, T.; Gevorgyan, V. *J. Org. Chem.* **2002**, *67*, 1936−1940.

(28) Buriak, J. M.; Stewart, M. P.; Geders, T. W.; Allen, M. J.; Choi, H. C.; Smith, J.; Raftery, D.; Canham, L. T. *J. Am. Chem. Soc.* **1999**, *121*, 11491−11502.

(29) Mewald, M.; Oestreich, M. *Chem.—Eur. J.* **2012**, *18*, 14079−14084.

(30) Harrison, D. J.; McDonald, R.; Rosenberg, L. *Organometallics* **2005**, *24*, 1398−1400.

(31) Parks, D. J.; Piers, W. E. *J. Am. Chem. Soc.* **1996**, *118*, 9440−9441.

(32) Zbigniew, J. L. In *Boron Science*; CRC Press: Boca Raton, FL, 2011; pp 3−20.

(33) Hessel, C. M.; Henderson, E. J.; Veinot, J. G. C. *Chem. Mater.* **2006**, *18*, 6139−6146.

(34) Yang, Z.; Dobbie, A. R.; Cui, K.; Veinot, J. G. C. *J. Am. Chem. Soc.* **2012**, *134*, 13958−13961.

(35) Smith, B. C. *Infrared Spectral Interpretation: A Systematic Approach*; CRC Press: London, 1998; pp 158−160.

(36) Delpuech, N.; Mazouzi, D.; Dupre, N.; Moreau, P.; Cerbelaud, M.; Bridel, J. S.; Badot, J. C.; De Vito, E.; Guyomard, D.; Lestriez, B.; Humbert, B. *J. Phys. Chem. C* **2014**, *118*, 17318−17331.

(37) Cheng, X.; Lowe, S. B.; Ciampi, S.; Magenau, A.; Gaus, K.; Reece, P. J.; Gooding, J. J. *Langmuir* **2014**, *30*, 5209−5216.

(38) Avramov, P. V.; Fedorov, D. G.; Sorokin, P. B.; Chernozatonskii, L. A.; Gordon, M. S. *Los Alamos Natl. Lab., Prepr. Arch., Condens. Matter* **2007**, 1−19.

(39) Regli, S.; Kelly, J. A.; Shukaliak, A. M.; Veinot, J. G. C. *J. Phys. Chem. Lett.* **2012**, *3*, 1793−1797.

(40) Wang, R.; Pi, X.; Yang, D. *J. Phys. Chem. C* **2012**, *116*, 19434−19443.

(41) Botas, A. M. P.; Ferreira, R. A. S.; Pereira, R. N.; Anthony, R. J.; Moura, T.; Rowe, D. J.; Kortshagen, U. *J. Phys. Chem. C* **2014**, *118*, 10375−10383.

(42) Oertle, K.; Wetter, H. *Tetrahedron Lett.* **1985**, *26*, 5511−5514.

(43) Asao, N.; Sudo, T.; Yamamoto, Y. *J. Org. Chem.* **1996**, *61*, 7654−7655.

(44) Houghton, A. Y.; Hurmalainen, J.; Mansikkamaki, A.; Piers, W. E.; Tuononen, H. M. *Nat. Chem.* **2014**, *6*, 983−988.